CIRSI Data Calibration

December 8, 1999

1 Introduction

We inspected calibration observations taken with CIRSI on 23 May 1999 and 24 May 1999 in Reset-Read-Read mode at Las Campanas to begin assessing possible instrumental artifacts in CIRSI data. In particular, we quantified the noise and spatial structure in dark and flatfield frames and looked for dependencies on detector number, loop number, run number, signal level, and exposure time. Our preliminary conclusions, some of which were already known, are:

- Loop 1 data should probably not be used because loop 1 dark and flatfield frames were not stable between consecutive runs. The ISAAC-SW Data Reduction Guide mentions an apparently similar problem. The SOFI User Manual mentions that stopping and restarting their array introduces an additional component to the signal that decays with time. Modifying Pixcel to do continuous read-out (but only storing frames when the user asks) could eliminate this problem.
- The flatfield frames show an odd/even effect, with sensitivity alternating between high and low with row number (with an amplitude of a couple percent). The CFHT Redeye Manual mentions a similar problem and suggests flatfielding to correct this. The division of CIRSI flatfield frames of similar signal levels did indeed remove this effect.
- The division of CIRSI flatfield frames of different signal levels did not yield a flat image (there was structure at the level of a couple of percent). This is apparently because the detectors have spatially dependent non-linearity, which is expected for infrared (X-Y addressable) arrays. However, the structure persisted when dividing frames with relatively low signal levels (e.g., 1200 / 700 dn), at which levels non-linearity effects were expected to be relatively insignificant. It is possible in RRR mode to be further along the linearity curve than realized (depending on the delay between the reset and first read), but this explanation seems unlikely given the 10 second exposure times.
- The dark frames contain structure on various scales at a level comparable to the read noise ($\approx$ 5 dn, $g = 10$ e$^-$/dn). The types of structure include large scale image gradients, sinusoidal pattern noise (image stripes), mean signal level offsets, warm/cool pixels ($\approx 3\%$), the "reset ramp", and the image cross (multiple bad rows and columns at the quadrant boundaries of all four detectors). Some of this structure appears to subtract out well, such as the reset ramp (which appears to be an additive effect) and the warm/cool pixels, while some does not (e.g., the sinusoidal pattern noise).

It is likely that none of these image features are unique to CIRSI. For example, the AAO IRIS User's Guide describes apparently similar types of cyclic pattern noise and odd/even effects (and suggests careful flatfielding), while the ARNICA Commissioning Report suggests that the image cross is an effect of quadrant read-out.

- The dark frame counts do not increase with exposure time (from 20 to 60 seconds), implying that either the dark current is not linear with time or it is too small to measure. If the dark current is too small to measure, what is the source of the ~ 15 dn signal level in the dark frames? Isn't the bias automatically removed in RRR mode?

We elaborate further on these conclusions in Section 2, and in Section 3 we describe a more systematic plan to obtain the necessary observations and measurements to characterize the detectors (i.e., the gain, read noise, dark current, bad pixels, and non-linearity properties).

2 Characterizing Dark and Flatfield Frames

2.1 Analysis Procedure

The raw calibration frames (`irx*fits`) that were inspected are in:

```
cass:/data/H_cass19d/cirsi/IoATime/19990524
cass:/data/mds13/aef/Experimental/19990523
cass:/data/mds13/meg/cirsi/darks/
```

Examples of dark and flatfield frames are shown in Fig. 1 and 2. The dark frames available have exposure times of about 20 to 60 seconds, and the flatfield frames have a signal level of about 700 to 8000 dn (but constant exposure time). We quantify the noise and spatial structure in each 512x512 image quadrant separately using the six plots shown in Fig. 3:

- the grey-scale image
- the image histogram, the number of low and high outliers (4σ), and the mean μ and standard deviation σ from a gaussian fit
- the image profiles in each direction (small circles), the profiles rebinned by a factor of 8 (plus signs), the parabolic fit to the profiles, the ramp amplitude A (the largest residual between the rebinned profile and the parabolic fit), and the large scale trend δ (the fit maximum $-$ fit minimum)
- the histogram of local standard deviations measured in a sliding 8x8 pixel box
- the mean standard deviation as a function of the size scale of the sliding box

Robust statistics are always used, e.g., outliers are clipped using the median and median absolute deviation.

2.2 Characterizing Dark Frames

The dark frames have image histograms that resemble a gaussian (σ = 6–8 dn, $g \approx 10$ e^{-}/dn), but with significantly broader wings (see Fig. 3). The histogram tail extends into negative dark counts due to read noise. About $\approx 0.5\%$ of the pixels are cool (dn $< \mu - 4\sigma$), and $\approx$ 2–4% are warm (dn $> \mu + 4\sigma$). Detector 3 (with the "boomerang" in flatfield frames) tends to have the most warm pixels. Loop 1 observations have less consistent behavior, with σ sometimes larger by about 20% and the number of cool pixels reaching 5%.

The mean signal level (histogram mean μ for a given quadrant) in four consecutive dark frames varied from about $\mu \approx 7$ to 20 dn without any obvious dependence on exposure time (20 to 60 seconds), quadrant number, detector number, or run number. For a given loop and quadrant, the mean signal level typically varied by 3–10 dn between the consecutive runs (up to a few times more for loop 1). The variation between consecutive loop numbers for a given run number was less (often only a couple dn, except for loop 1 to 2 which varied by $\sim$ 10 dn).

Several types of structure were noticed in the dark frames:

- Large scale trends in the dark frames of $\delta \approx 1$ to 10 dn are common. For a given loop number and quadrant, the δ varied between consecutive runs by a few dn, often twice as much for detector 3, and several times as much for loop 1. The variation with loop number for a given quadrant and run was significantly less (except for loop 1 to 2).

- There are small scale cyclic patterns, including sinusoidal image stripes (amplitude of $\sim$ 5 dn) and sometimes a smaller amplitude odd/even effect (alternating high and low signal levels in consecutive image rows). These effects can be seen in the grey scale image (Fig. 1), but they are much more blatant in a smoothed version of the image profile (Fig. 4). The sinusoidal profile pattern is not eliminated by subtracting two darks of the same loop and different run number (Fig. 5 and 6). The sinusoidal profile persisted in subtractions of darks with the same run but different loop.

- There is a "reset ramp," which manifests as a sharp rise in counts in the first 10–20 rows of each quadrant (or columns depending on the image rotation). The amplitude of the ramp is typically about $A \sim 10$ dn. The ramp does not appear to be a multiplicative effect because it can go below 0 in the image profile (Fig. 7), and the amplitude does not seem to depend on the mean signal level (5–15 dn). In flatfield images with thousands of counts there is no obvious equivalent ramp structure. The ramp amplitude is the same (within $\sim$ 1 dn) for a given quadrant and loop number at different consecutive runs. The amplitude does not seem to depend on loop number much either. The ramp seems to subtract out well (Fig. 8).

- There are hot rows and columns that form a cross at the quadrant boundaries (about 2–3 pixels wide). This occurs on all four chips. In flatfield frames part of this structure can appear at negative N thousand counts instead of N thousand.

To characterize the noise level we measured robust standard deviations in an 8x8 sliding box. The histogram of these local deviations does not resemble a gaussian but rather is strongly asymmetric (e.g., Fig. 3, bottom left). In other words, the measured scatter in the dark frames is a strong function of position in the image quadrant, ranging from about 4 to 15 dn ($g = 10.17$ e^{-1}/dn). The direction of the noise gradient appears to rotate 90 degrees from one chip to the next, but this is just because the data were rotated by the online software (Pixcel). The difference of two dark frames yields a gaussian noise histogram (with a mean noise level of about 5.5 dn) and a gaussian image histogram (e.g., Fig. 8). Also, flatfield images have a gaussian error histogram. Thus the noise gradient appears to be the result of cool/warm pixels that are not randomly positioned.

2.3 Characterizing Flatfield Frames

The flatfield frames were analyzed using the same procedure as the dark frames. An example plot is shown in Fig. 9. The image quadrant has a mean signal level of about 6600 dn, with a 1σ sensitivity variation of about 3% (typically about 6% for detector 3). For all four detectors the mean signal level agreed between loops to better than 1%, except for loop 1 which had systematically fewer counts by about 5–10%.

The image profiles suggest that the sensitivity is relatively flat (within about 10%), except for detector 3 with the famous boomerang structure (e.g., Fig. 10). Selecting pixels with a sensitivity that deviates by more than 25% from the median yields a map of likely bad pixels (Fig. 11). All four detectors show a sensitivity that alternates by a few percent with row number (i.e., the odd/even effect indicated by the distinct high and low Y Profiles in Fig. 9).

When a flatfield frame is divided by another flatfield frame of similar mean signal level, the image profiles of the result are flat to better than about 0.1% on all four detectors (e.g., Fig. 12). At lower signal level ($\sim$ 1000 dn), however, the divided frames often had increased structure ($\delta = 0.1$ to 1%, e.g., Fig. 13). When the signal levels of the flatfield frames being divided differ, the result is structure δ in the image profiles at the 1–5% level (Fig. 14). The effect was larger (3–5%) for the two pairs of frames with lower average signal levels (about 1000 dn). When the quotient of one pair of flats was divided by the quotient of an independent pair of flats (both with the same signal ratios), the result was a structureless image.

3 Characterizing the CIRSI Detectors

In this section we describe a plan to characterize the CIRSI detectors (gain, read noise, dark current, and non-linearity properties) using a set of calibration frames to be taken in November 1999.

We will take a series of dome flats (constant lamp brightness) and darks with increasing exposure times and numerous loops at each exposure time. The exposure times are varied to give count levels in the flats from a few hundred counts to saturation, and dark exposures long enough to measure the dark current and its non-linearity with time up to the longest science observations. Between each dome flat, a reference frame of fixed exposure time will be taken to monitor the source flux.

We will fit a curve to the signal vs. exposure time for each pixel in the darks and flats to determine dark current as a function of time and position, and signal level as a function of brightness, position, and color (an image of each fit coefficient). We will apply the variance method to the variance vs. signal plot to calculate the gain factor and the read noise.

Of course, this was only the 10 second version of the plan, and it will be improved.

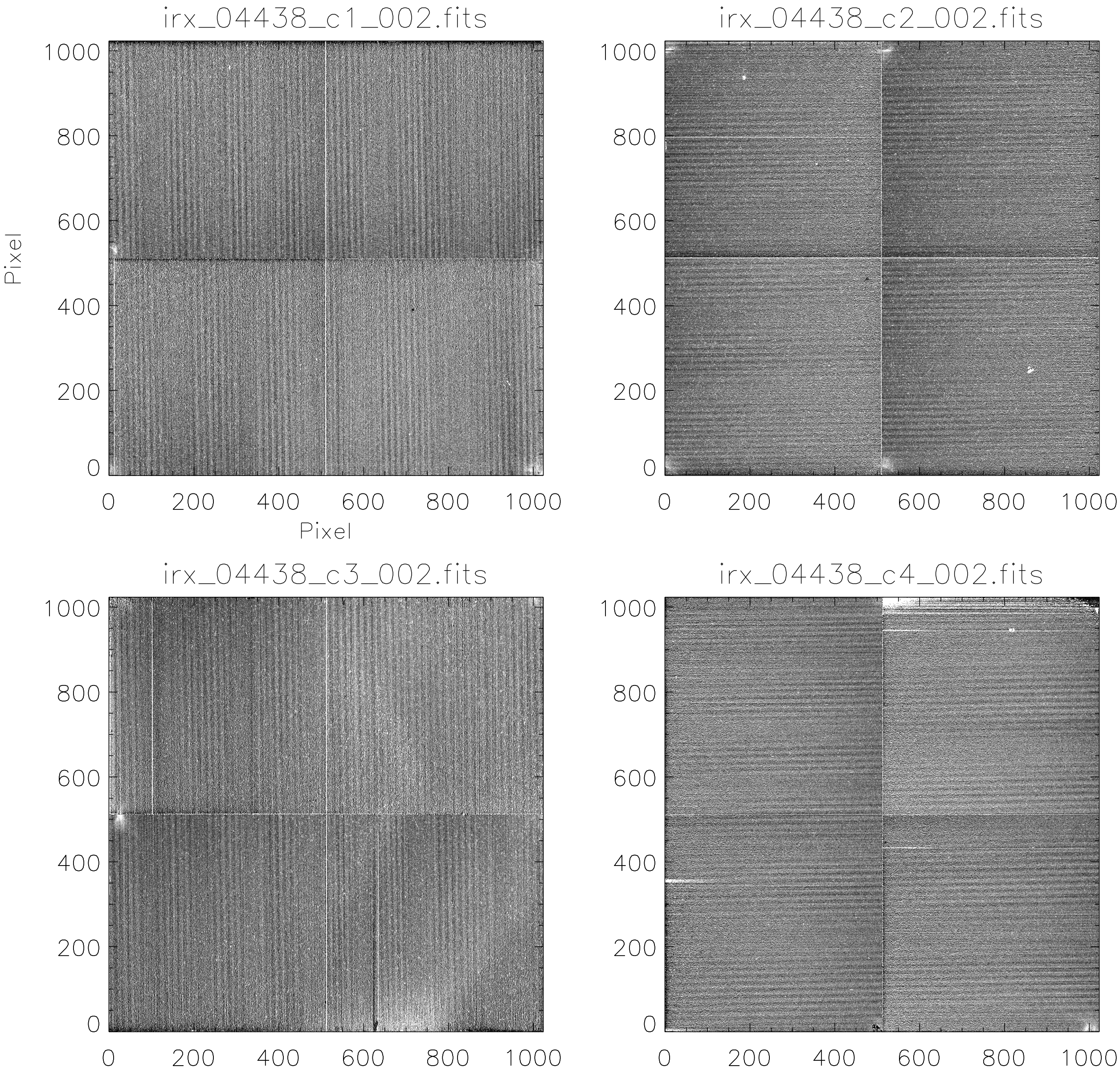

Figure 1: A 23 second dark observation taken with the CIRSI mosaic of four 1Kx1K detectors on 24 May 1999 at Las Campanas. The observation was taken in RRR mode (correlated double sampling). The mean signal level is about 15 dn.

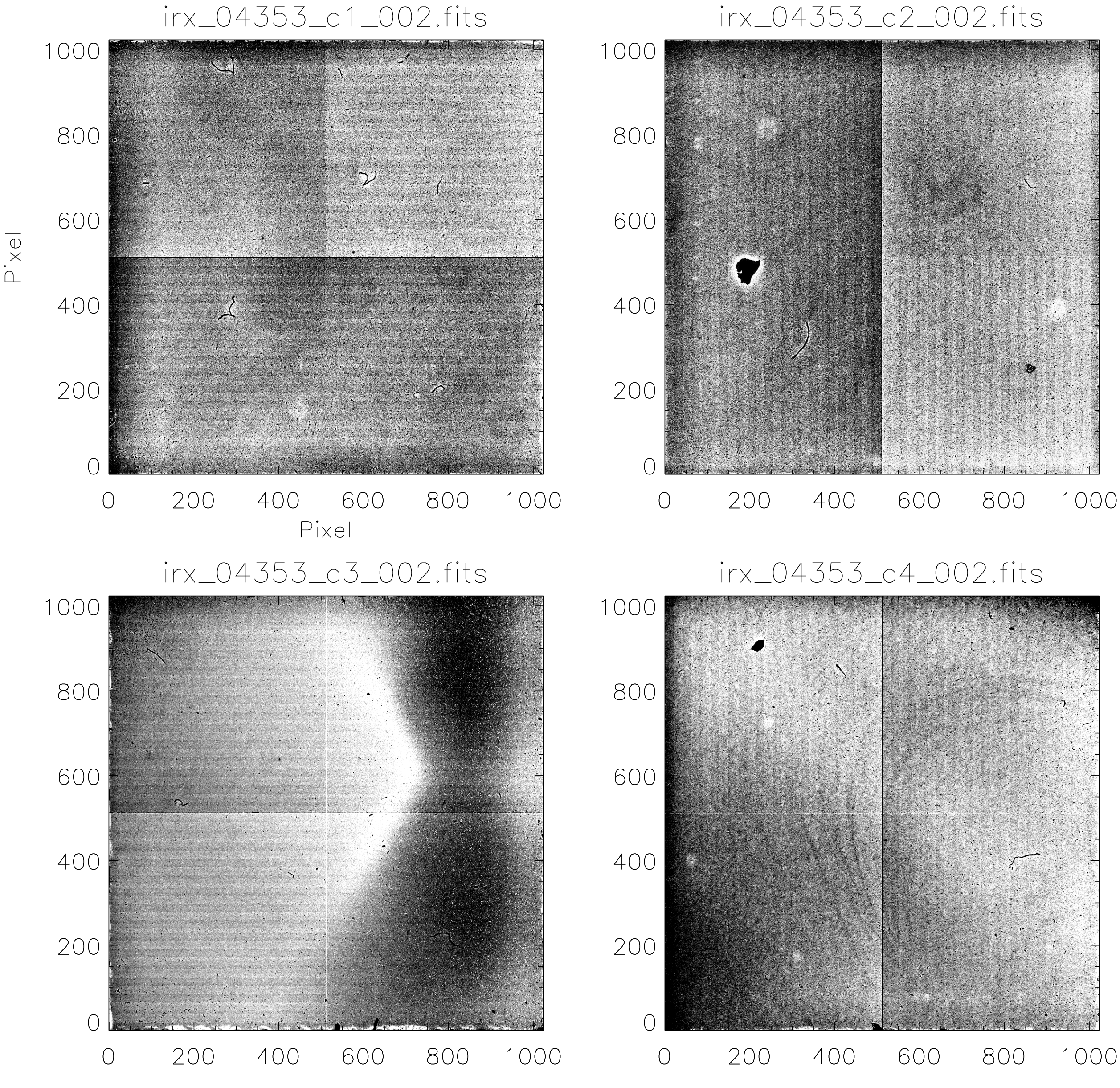

Figure 2: A domeflat observation taken with the CIRSI mosaic of four 1Kx1K detectors on 23 May 1999 at Las Campanas. The observation was taken in RRR mode. The mean signal level is about 6000 dn.

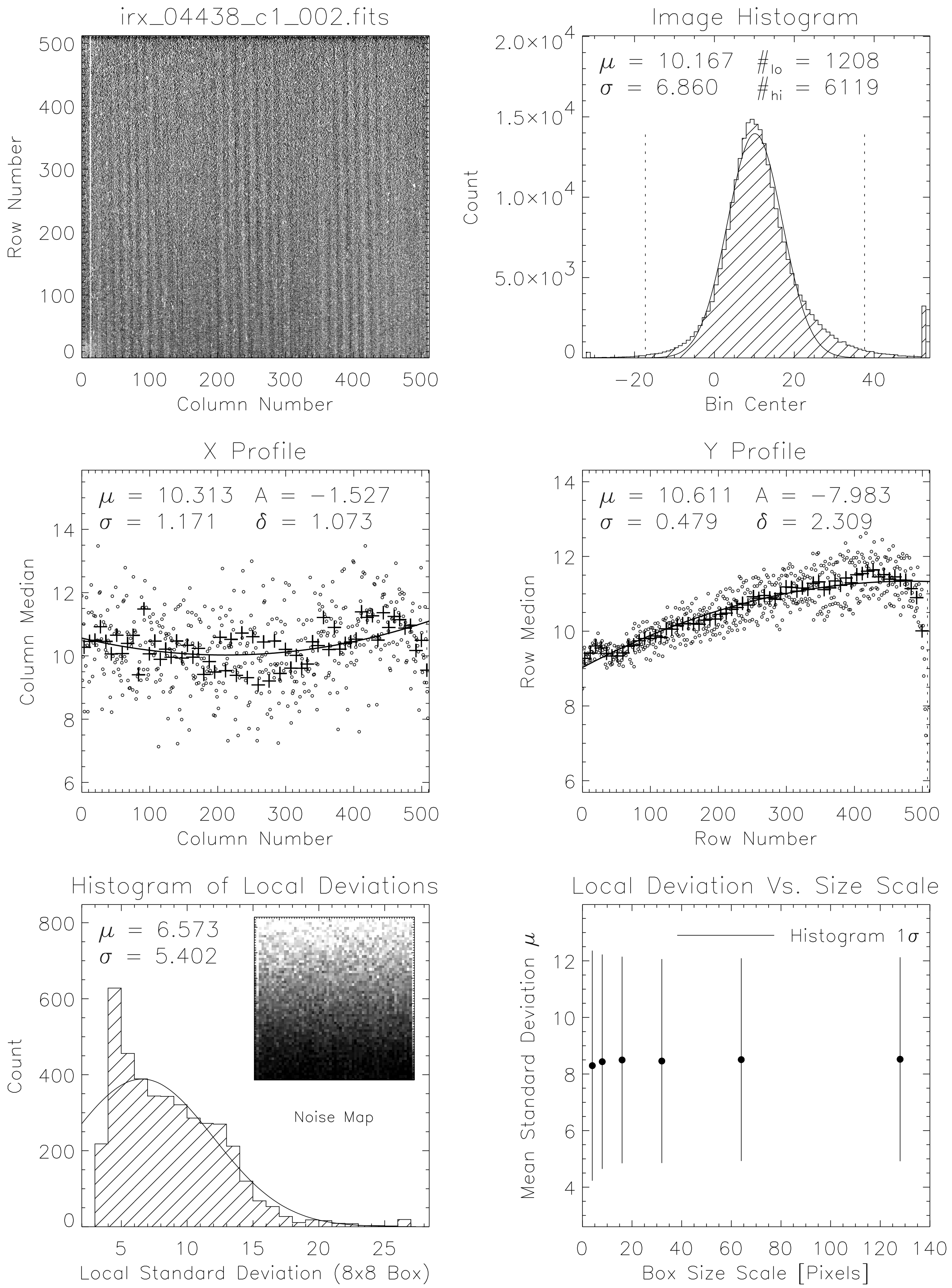

Figure 3: The analysis of a dark frame (the first quadrant of the first detector) is shown. The observation was taken in RRR mode with a 23 second integration time.

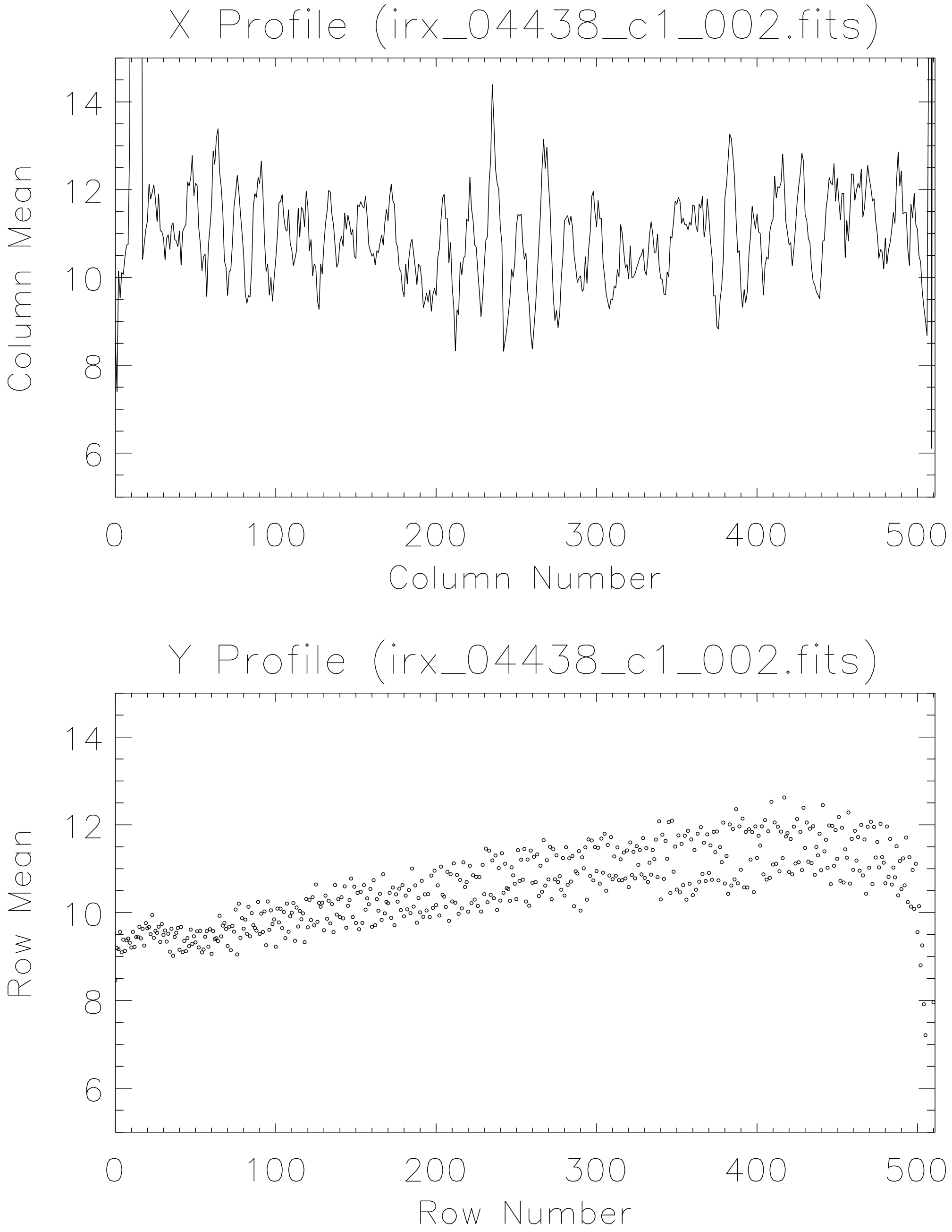

Figure 4: On top is shown the image profile looking along columns over a restricted range of rows with box car smoothing of 7 pixels (the sinusoidal pattern noise). On the bottom is the profile looking along rows (the odd/even effect is sometimes seen in dark frames).

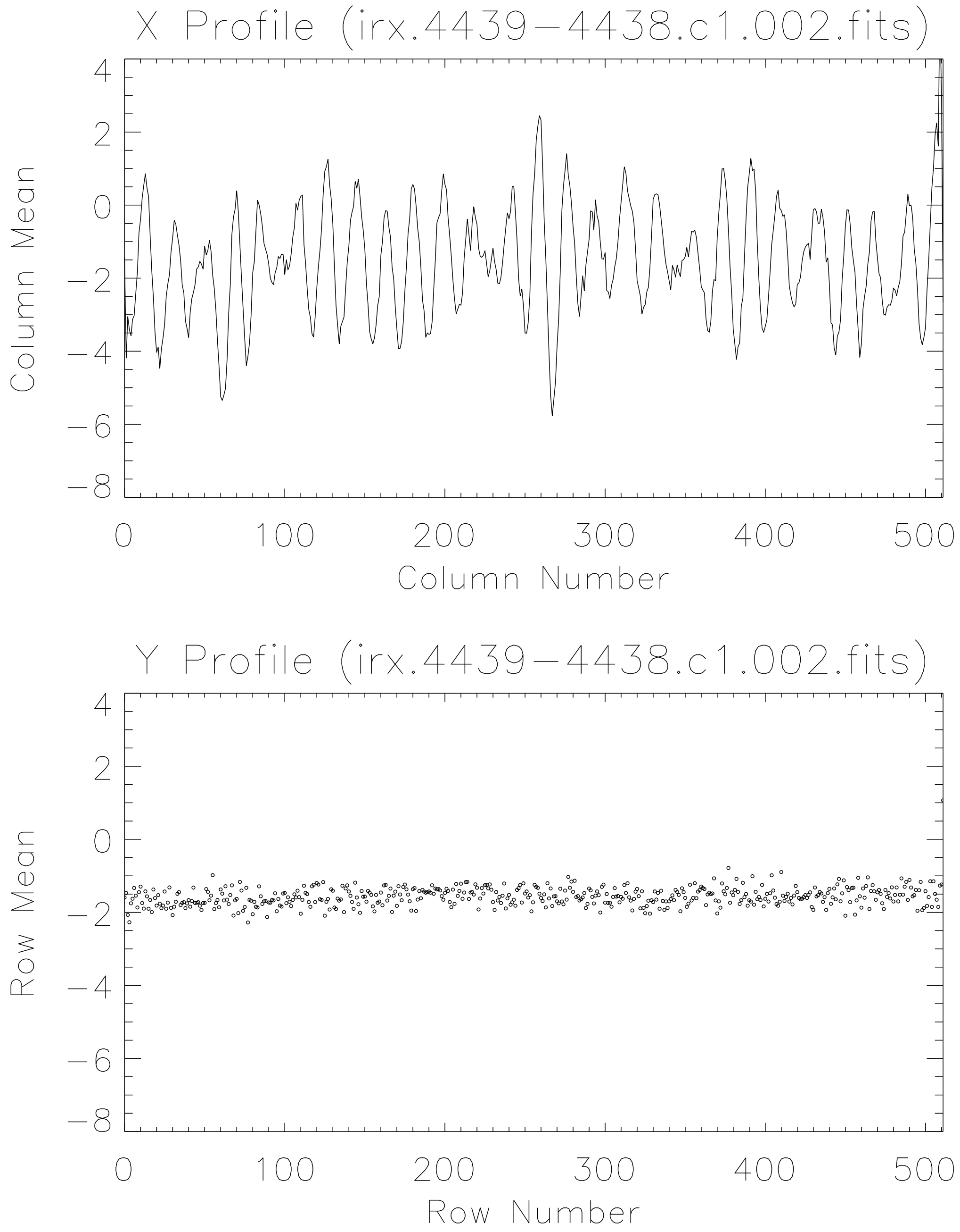

Figure 5: The same as the previous figure, but using the difference of two dark frames for a given loop (2) but different (consecutive) run numbers.

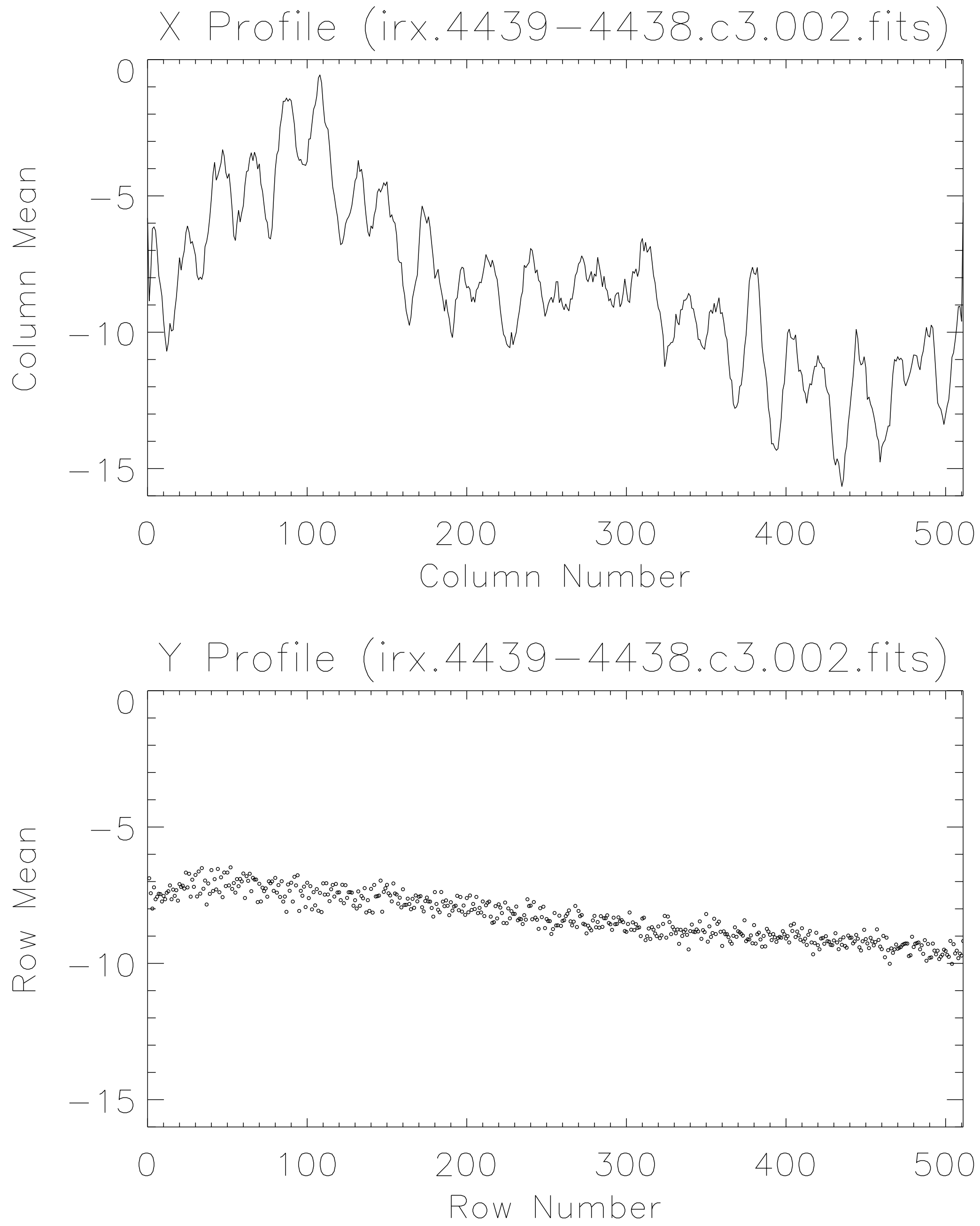

Figure 6: The same as the previous figure, but a residual large scale trend that did not subtract out well is superimposed.

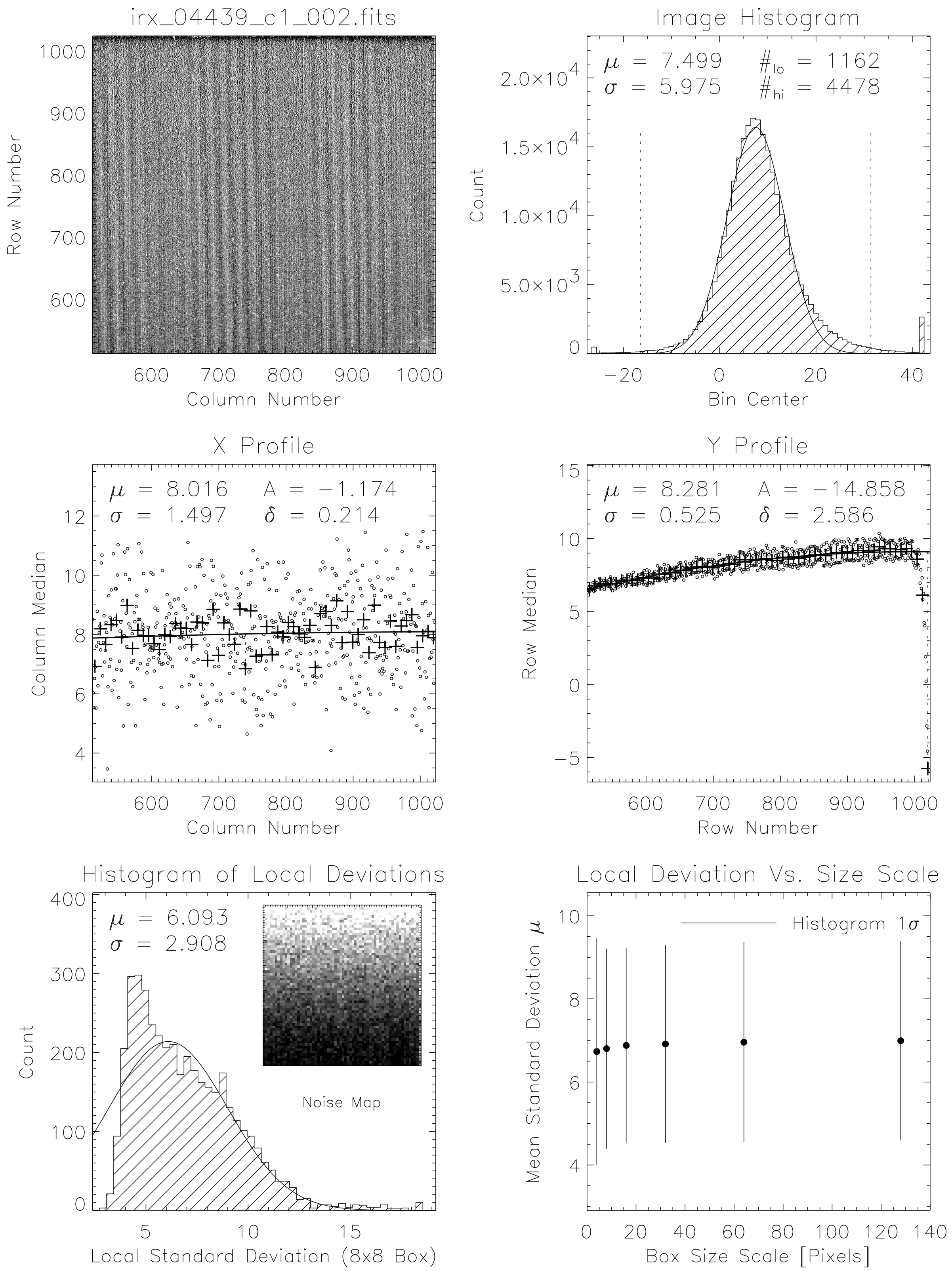

Figure 7: The analysis of a dark frame quadrant. The Y Profile shows that the reset ramp (near row 1000) can go negative. This is one of the reasons that the ramp does not seem to be a multiplicative effect.

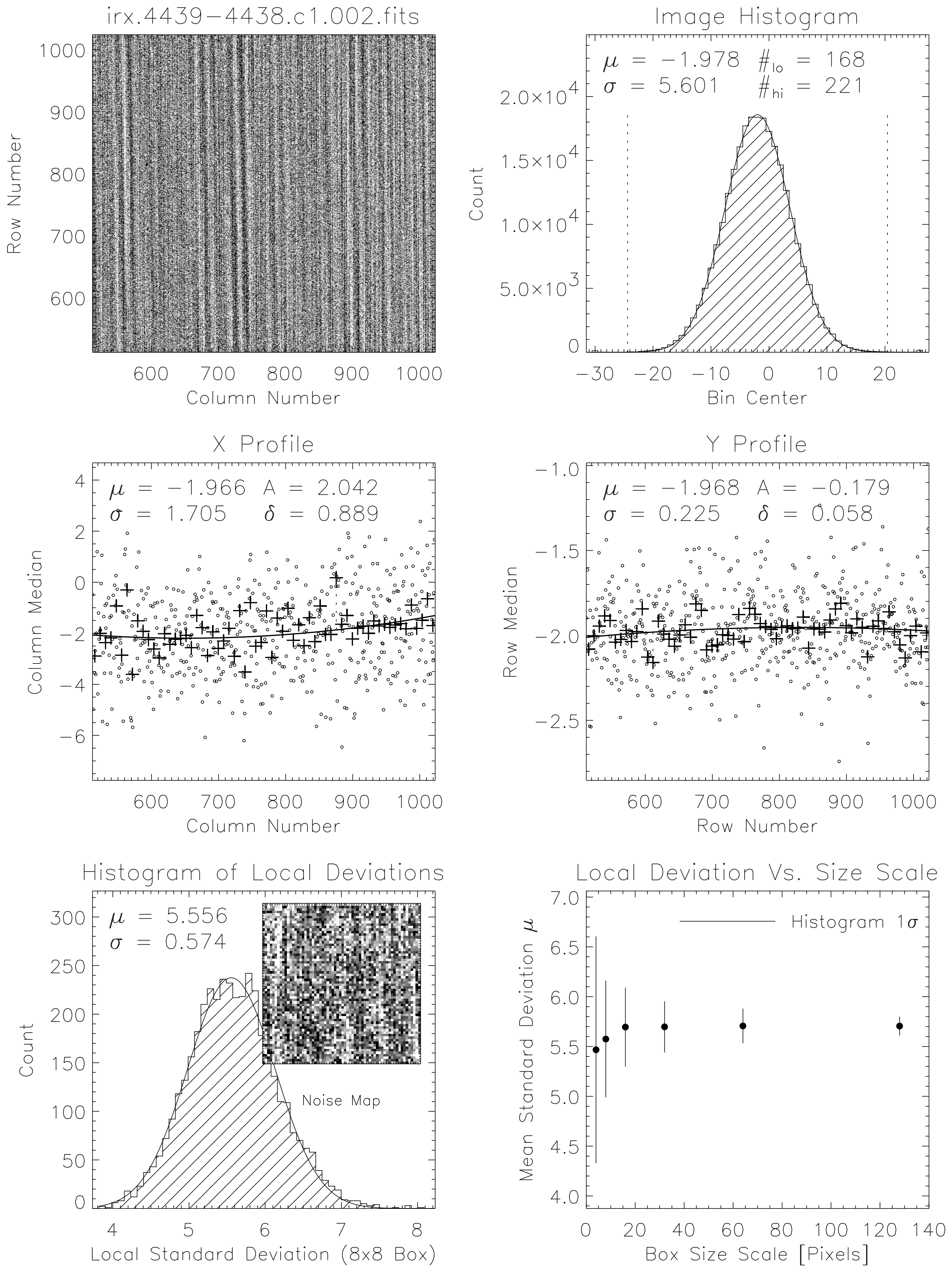

Figure 8: The reset ramp normally seems to subtract out well. The difference of two dark frames (same loop, different run) is shown.

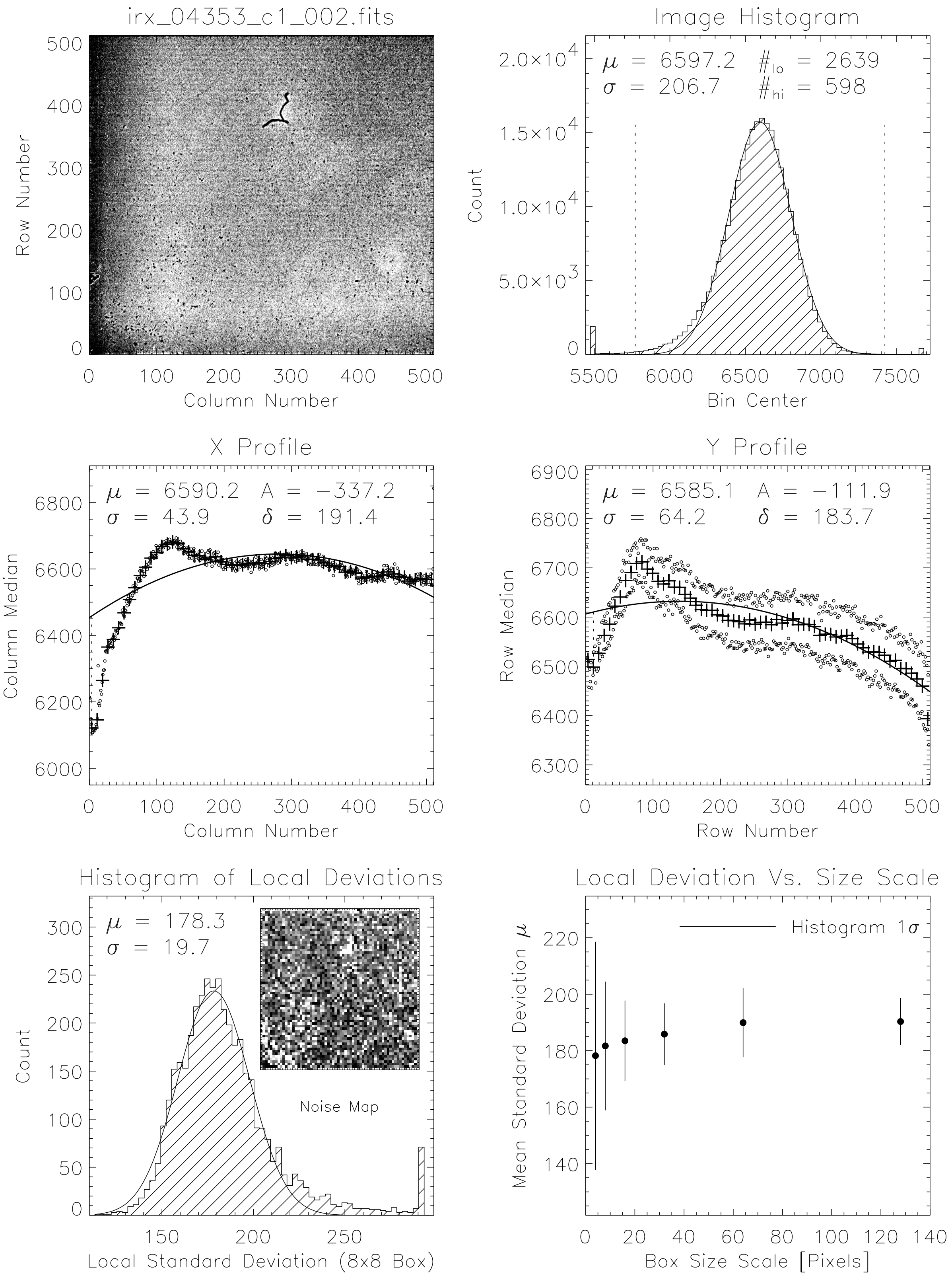

Figure 9: The flatfield frames were analysed using the same procedure as the darks. An example is shown.

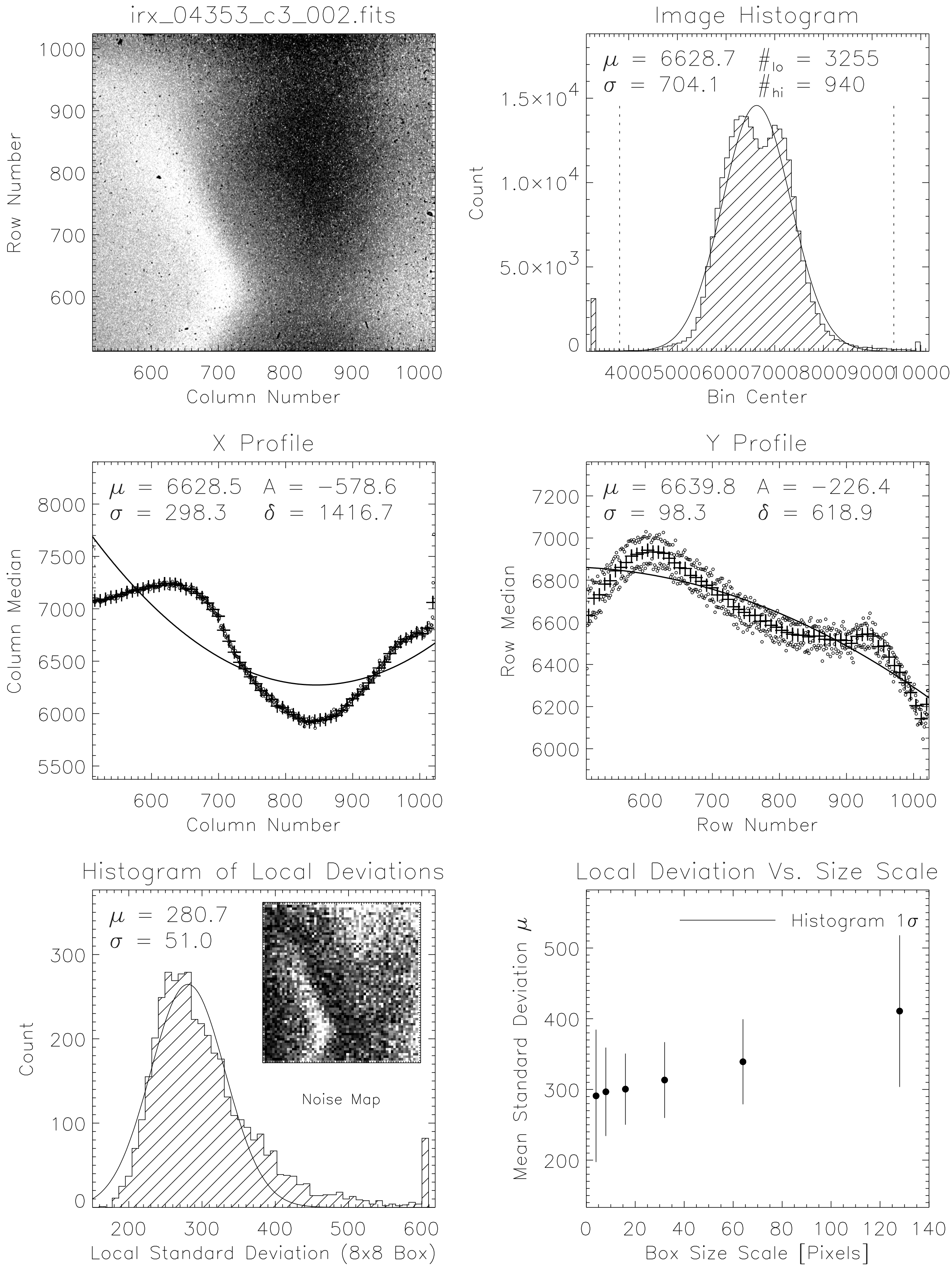

Figure 10: The famous boomerang structure on detector 3. The sensitivity fluctuates more than the other detectors.

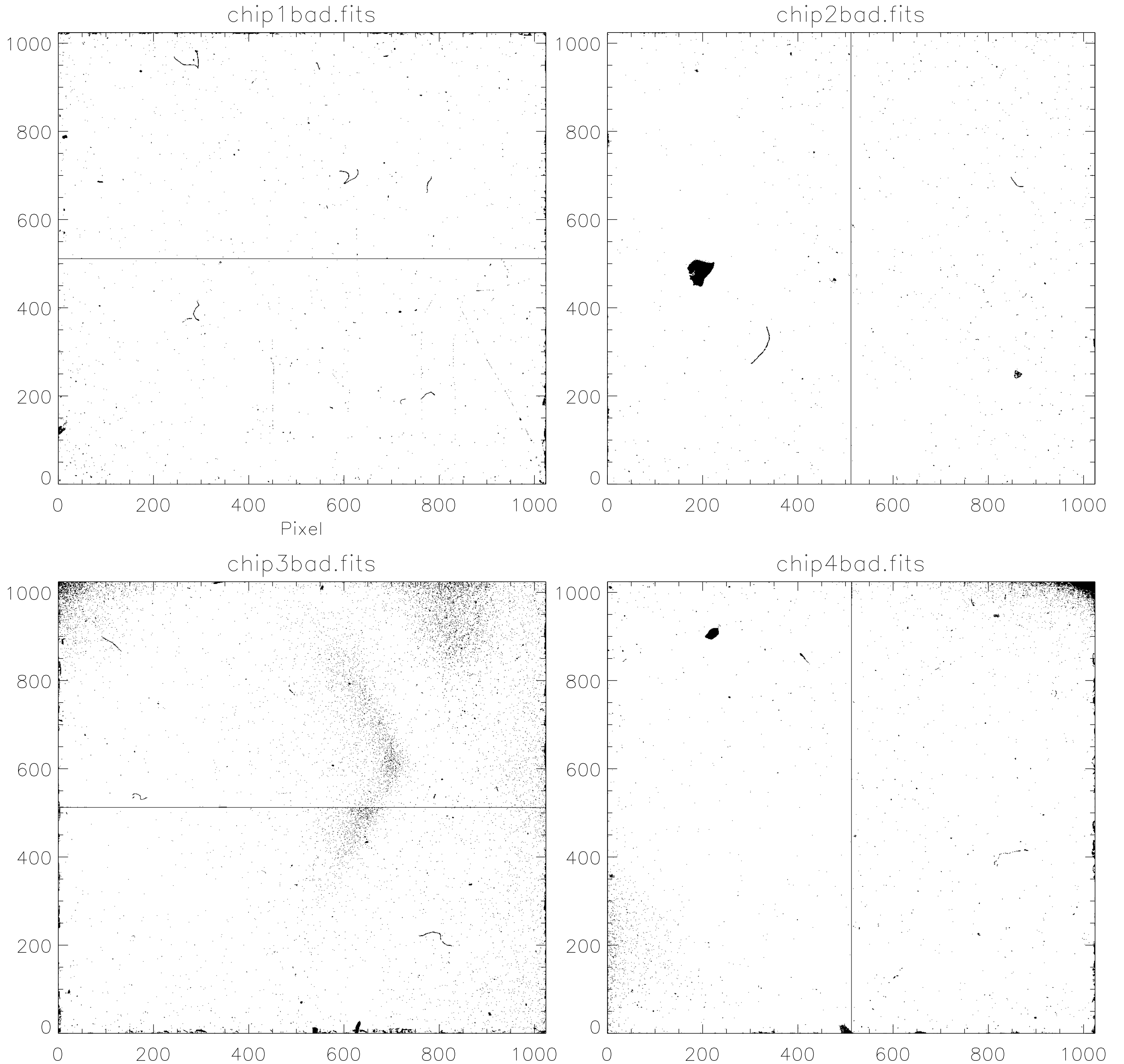

Figure 11: A bad pixel map was produced by selecting pixels with sensitivity that deviates by more than 25% from the median sensitivity.

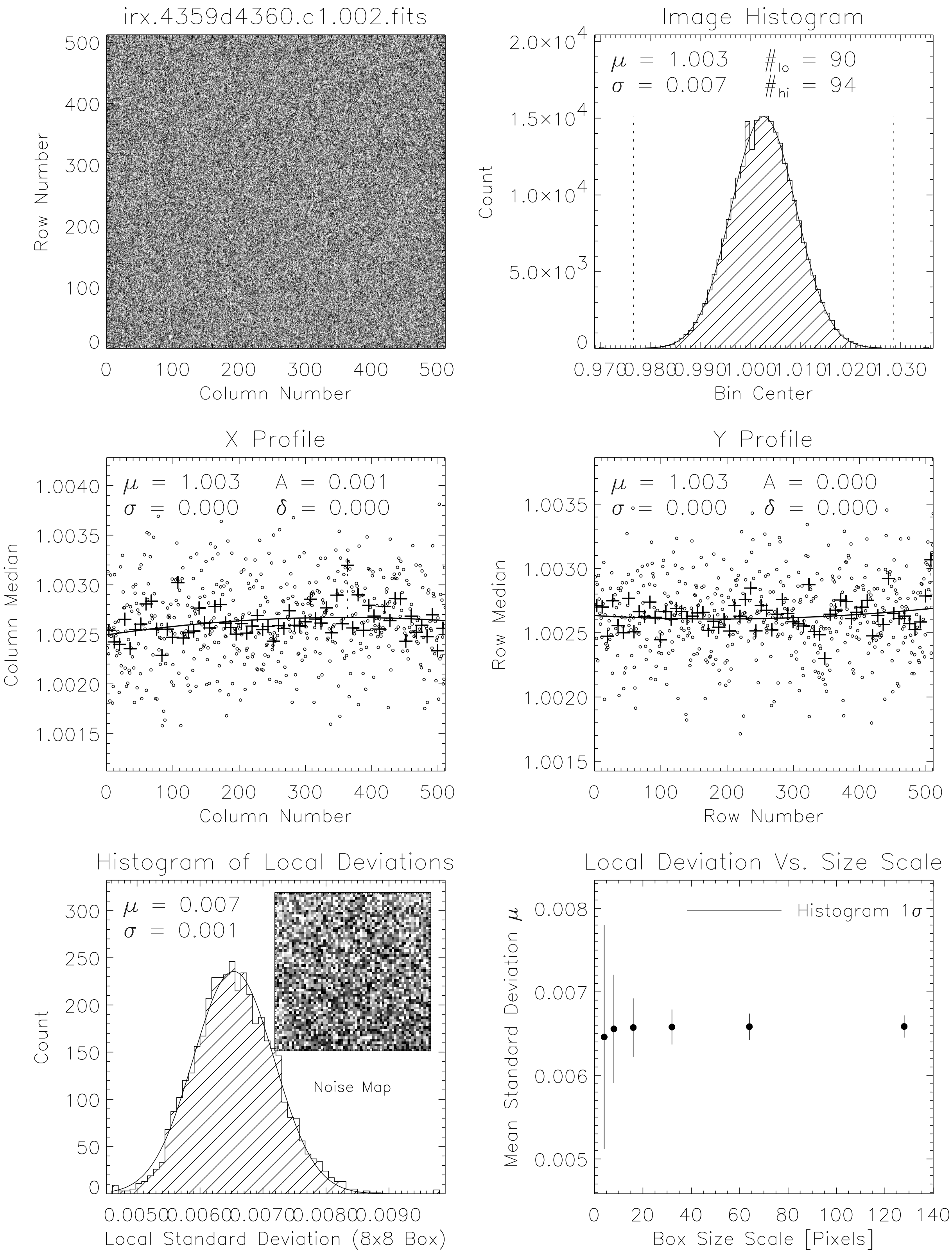

Figure 12: Two flatfield frames of similar mean signal level were divided and analysed. The image profiles of the result are flat to better than about 0.1% on all four detectors. For pairs of flatfields at lower signal levels (~ 1000 dn), there was sometimes increased structure ($\delta = 0.1$ to 1%, see next figure).

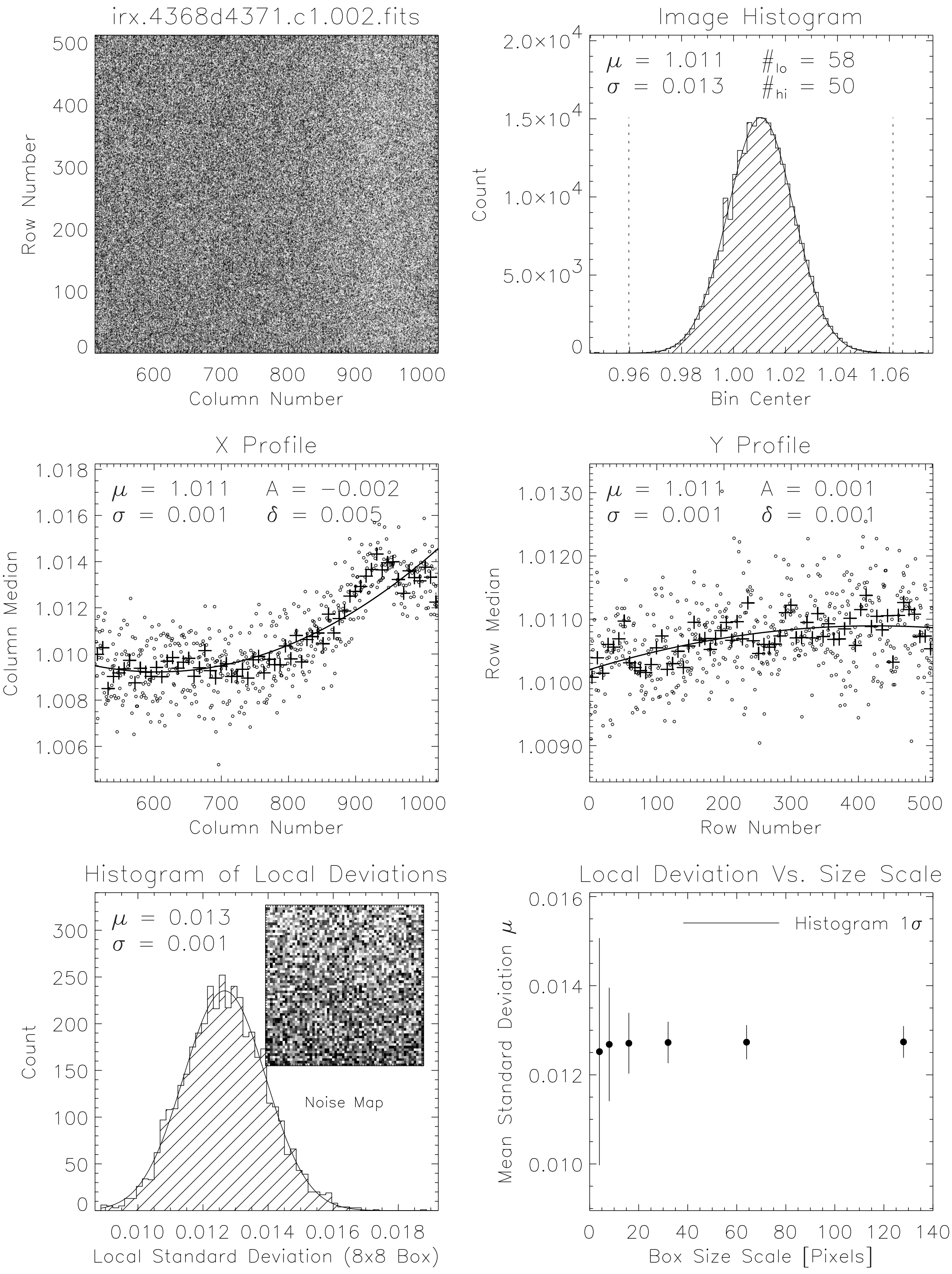

Figure 13: When dividing flatfield frames of similar mean signal, there was increased structure (δ = 0.1 to 1%) for the two pairs of frames with lower mean signal levels ($\sim$ 1000 dn).

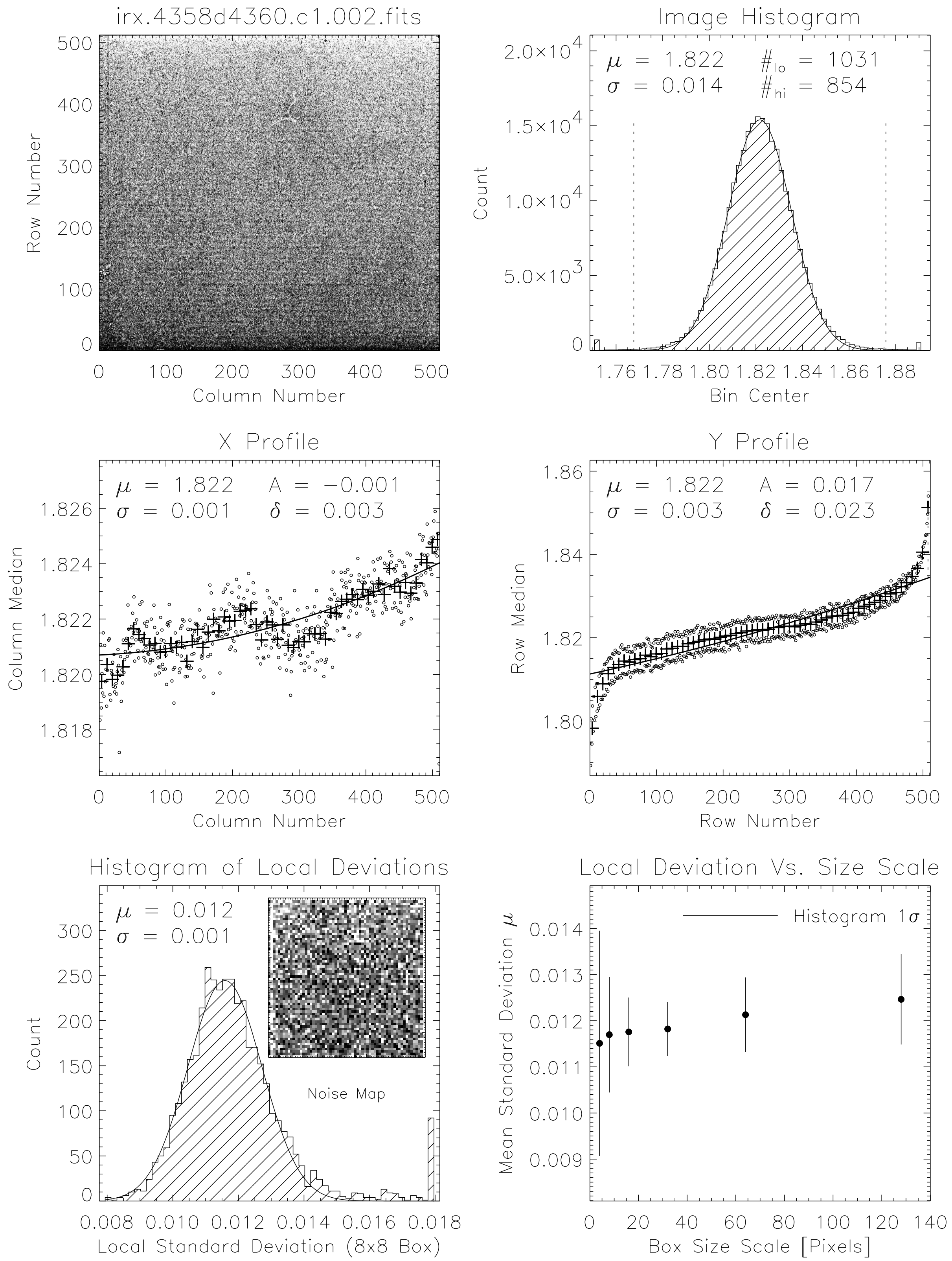

Figure 14: When the signal levels of the flatfield frames being divided differ, the result is structure δ in the image profiles at the 1–5% level.